

## A Model for the Thermodynamic Growth of Sea Ice in Numerical Investigations of Climate

ALBERT J. SEMTNER, JR.<sup>1</sup>

*Climate Dynamics Program, Rand Corporation, Santa Monica, Calif. 90406*

(Manuscript received 11 July 1975, in revised form 27 December 1975)

### ABSTRACT

A model is presented whereby the thickness and extent of sea ice may be predicted in climate simulations. A basic one-dimensional diffusion process is taken to act in the ice, with modifications due to penetration of solar radiation, melting of internal brine pockets, and accumulation of an insulating snow cover. This formulation is similar to that of a previous study by Maykut and Untersteiner, but the introduction of a streamlined numerical method makes the model more suitable for use at each grid point of a coupled atmosphere-ocean model. In spite of its simplicity, the ice model accurately reproduces the results of Maykut and Untersteiner for a wide variety of environmental conditions. In 25 paired experiments, annual average equilibrium thicknesses of ice agree within 24 cm for 75% of the cases; and the average absolute error for all cases is 22 cm. The new model has fewer computational requirements than one layer of ocean in the polar regions, and it can be further simplified if additional savings of computer time are desired.

### 1. Introduction

Increasing attention is being paid to the problem of predicting variations in climate due to natural or man-made causes. Of the many components in the climatic system, sea ice is probably a very important one. It has the potential of amplifying climatic variations on account of two positive feedback mechanisms. First, the formation of ice reduces heat transfer between the ocean and atmosphere, inhibiting the ocean's normal ability to moderate climate through local seasonal heat storage and lateral heat transport. Second, the formation of ice causes a much larger portion of the incoming solar energy to be reflected back to space. In both cases, a colder atmosphere and further ice growth may result. In view of these effects, the proper prediction of the sea ice would seem to be an important requirement in modeling climate.

A number of physical processes govern sea ice. The best understood of these, and probably the most important, involves the vertical growth and decay of individual ice sheets in response to energy fluxes at the upper and lower surfaces. A time-dependent vertical diffusion process acts within the ice, modified by effects of internal heating due to penetrating solar radiation and internal storage of heat in brine pockets. It is this vertical diffusion process which has been simulated in a definitive model by Maykut and Untersteiner (1969, 1971) and which is simplified here for use in climate models.

Dynamical effects can also influence the sea ice cover. For example, if the motion field of the pack ice is divergent (as it often is in the Southern Ocean), ice may be transported into zones where it might not occur by thermodynamic processes alone. The open spaces left behind as leads within the pack ice are likely to freeze over in winter, with a resultant increase in the total area covered by ice. During the summer, however, such leads are likely to enlarge through the absorption of solar radiation, causing a more rapid reduction in ice coverage than might otherwise occur.

The complicated dynamics of pack ice and its interaction with sea-ice thermodynamics are now being studied intensively by the Arctic Ice Dynamics Joint Experiment. Improvements on a purely thermodynamic treatment of sea ice will undoubtedly arise out of AIDJEX. However the vertical thermodynamic process (possibly for multiple species of ice) should retain a central role. Thus, the simple thermodynamic model described here may be usable as an important component of a more general model.

There is some indication now that much of the seasonal variation in sea ice extent can be accounted for by thermodynamics alone. In a recent study by Washington *et al.* (1976), the simple thermodynamic model proposed in the Appendix of this paper was used with observed forcing to predict reasonable seasonal variation of sea ice in the Arctic and Antarctic Oceans. The results indicate that a pure thermodynamic ice model may be adequate for use in climate modelling, at least until such time as highly sophisticated treatments of

<sup>1</sup>Permanent affiliation: Department of Meteorology, University of California, Los Angeles 90024.

other important climatic variables (e.g., clouds) are also developed.

## 2. Formulation of the model

The physical formulation of the model is a simplification of that used by Maykut and Untersteiner (1969, hereafter referred to as M&U). Sea ice is assumed to be a horizontally uniform slab of ice, on which snow can accumulate seasonally. The temperature within the snow cover is governed by the one-dimensional heat equation

$$(\rho c)_s \frac{\partial T}{\partial t} = k_s \frac{\partial^2 T}{\partial z^2}. \quad (1)$$

Values for the constants are  $k_s = 7.4 \times 10^{-4} \text{ cal cm}^{-1} \text{ s}^{-1} \text{ }^\circ\text{C}^{-1}$  and  $(\rho c)_s = 0.165 \text{ cal cm}^{-3} \text{ }^\circ\text{C}^{-1}$ . These are appropriate empirical values obtained from M&U for snow which is not melting. Unlike the formulation of M&U, no change in the values is made for melting snow, because melting occurs for a relatively short time, during which conductive fluxes are usually small. The temperature within the ice is governed by a similar equation

$$(\rho c)_I \frac{\partial T}{\partial t} = k_I \frac{\partial^2 T}{\partial z^2}. \quad (2)$$

For the constants, we use the M&U values appropriate for ice of low temperature, namely  $k_I = 4.86 \times 10^{-3} \text{ cal cm}^{-1} \text{ s}^{-1} \text{ }^\circ\text{C}^{-1}$  and  $(\rho c)_I = 0.45 \text{ cal cm}^{-3} \text{ }^\circ\text{C}^{-1}$ . Maykut and Untersteiner allow the values of these constants to change as a function of temperature for an assumed salinity profile within the ice. Their prescribed change in specific heat capacity is particularly dramatic as the melting temperature of ice is approached, and simulates the summer storage of heat in enlarging brine pockets trapped within the ice. They also add a heat source term in Eq. (2) to account for a fraction of the incoming solar radiation which penetrates into the ice and is absorbed exponentially with depth. The penetration of radiation occurs only when the ice is snow-free.

Penetrating solar radiation has been shown by the experiments of M&U to have an important effect on ice thickness, and thus it is desirable to include it even in a simple model. The penetrating radiation represents energy which is not available for producing immediate surface melting and runoff. Instead, this energy first warms the subsurface interior of the ice and then initiates melting of interior patches of high salinity ice (which exist as a natural consequence of brine rejection during the initial formation of the ice from sea water). Since conductive fluxes are usually small during the time when brine pockets are growing in size, virtually all this internal melting must be due to the penetrating radiation. The enlarging pockets of liquid remain trapped in the lattice of ice unless considerable melting takes place. They represent a stored quantity

of heat which has not been used to decrease the thickness of ice. With the onset of surface cooling in late summer, these pockets will give up heat as they freeze, keeping the subsurface interior near the freezing point until the heat is exhausted. However, this heat of fusion can be extracted fairly quickly because it is concentrated near the top of the ice. By mid-autumn, the heat supply is usually exhausted, and accumulation of ice at the lower boundary can begin. This accumulation takes place on ice which is thicker than it would otherwise be if all solar radiation had been applied toward surface melting.

In the present study, a simple formulation is used for the absorption of penetrating radiation and the increase in trapped brine volume. The formulation adapts more easily to a numerical scheme with low resolution than does the formulation of M&U, and it is more consistent than theirs in terms of overall energy conservation. During snow-free periods, the fraction of penetrating radiation is stored in a heat reservoir, which represents internal meltwater. Energy from this reservoir is used to keep the temperature near the top of the ice from dropping below the freezing point (unless the reservoir is exhausted), thereby simulating release of heat through refreezing of the internal brine pockets. The net result is that penetrating solar energy does not cause immediate surface melting in summer but does retard internal cooling in the fall.

Some limitation must be set on the amount of internal melting that can occur. (Otherwise, a situation could arise for a case with thin ice where more heat was stored internally than was needed to melt all the ice.) The heat storage reservoir is arbitrarily prevented from accumulating more than 30% of the amount needed to melt all the ice. When this maximum is reached, the heat of fusion at the top of the ice is dropped by 30% and heat from the storage reservoir (which represents ice already melted) supplies the remainder. Also the fraction of penetrating radiation is set to zero, so that no heat will remain in the reservoir if all the ice melts.

The boundary conditions for Eqs. (1) and (2) are identical to those of M&U. At the top of the snow (or ice, if no snow is present), a balance of fluxes is assumed to exist, unless such a balance would force the surface temperature to be above the melting point ( $0^\circ\text{C}$  for snow and  $-0.1^\circ\text{C}$  for ice). In that case, the imbalance of fluxes causes melting. Taking into account an ice density of  $0.9 \text{ g cm}^{-3}$  and a snow density of  $0.33$ , volumetric heats of fusion are  $se'$  at  $72 \text{ cal cm}^{-3}$  for ice and  $26.2 \text{ cal cm}^{-3}$  for snow. At the internal snow-ice interface, diffusive fluxes on both sides of the interface must be equal. Finally, at the bottom of the ice, any imbalance between a specified oceanic heat flux and the diffusive flux within the ice causes ice to accrete onto the bottom or to ablate from it. To allow comparison with the case studies of M&U, a somewhat

reduced heat of fusion ( $64 \text{ cal cm}^{-3}$ ) is used at the bottom of the ice. (Maykut and Untersteiner chose this value for heat of fusion at the lower boundary on the grounds that newly formed ice retains a liquid brine volume of about 10%. However, their treatment implies that an additional loss of heat over what is prescribed in surface fluxes must occur before the ice reaches the upper surface.)

An ice model for climatic simulation must be able to handle seasonal transitions between an ice-covered and an ice-free ocean. For this study, it is assumed that a mechanically driven oceanic mixed layer 30 m thick exists below the ice. If sea ice disappears, a heat budget equation for this vertically isothermal layer is applied until the layer again reaches the freezing point, at which time ice reappears. In a general climate study, inputs of heat at the sides and bottom of this layer would be predicted by an ocean model; but here their net effect is taken to be the specified oceanic heat flux.

### 3. Numerical scheme

The numerical scheme employed here is considerably different from that of M&U. Maykut and Untersteiner use very high resolution, presumably in order to resolve the absorption of penetrating radiation and predict summer ice minimum thicknesses down to only a few tens of centimeters. For their fixed grid-point separation of 10 cm, about 40 grid points are usually required. Because of the high resolution, a complicated differencing scheme (resembling an implicit method) is needed to allow a long time step.

In the present study, only about one-tenth as many grid points are used; one point lies in the snow and two lie evenly spaced within the ice. The number of ice points remains the same, even though the ice thickness varies, by virtue of an algorithm that continually changes the resolution. Because of the coarser resolution, a simple forward-differencing scheme can be used without unduly restricting the time step. (When the ice becomes very thin, the number of layers can be reduced, as will be discussed later in this section.)

Fig. 1 shows the grid arrangement and a typical temperature profile when two temperature points are carried within the ice. (For generality, however, we write down prediction equations for the case of  $n$  ice layers.) The temperature  $T_0$  is predicted for a snow layer of thickness  $h_s$ ; and temperatures  $T_1, \dots, T_n$  are predicted for ice layers of thickness  $h_I/n$ . Each temperature represents a value at the mid-point of its grid box. Conductive fluxes  $F_k$  across interior interfaces are based on an assumed linear temperature profile between grid points, so that

$$F_k = k_I \frac{T_{k+1} - T_k}{h_I/n}, \text{ for } k=1, \dots, n-1.$$

(In this and in subsequent equations, fluxes are taken

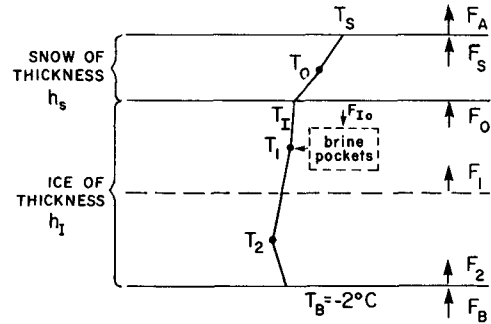


FIG. 1. Schematic diagram of the 3-layer model. Temperatures in the layers and thicknesses of the snow and ice are predicted on the basis of fluxes across internal and external boundaries. Energy of penetrating radiation is stored in brine pockets and released during freezing.

to be positive upward.) The conductive flux  $F_n$  at the bottom of the ice is obtained similarly, using a constant bottom temperature  $T_B = -2^\circ\text{C}$ :

$$F_n = k_I \frac{T_B - T_n}{h_I/2n}.$$

At the snow-ice interface, a temperature  $T_I$  is employed which satisfies a conductive flux balance condition. The flux is given by

$$F_0 = k_I \frac{(T_1 - T_I)}{h_I/2n},$$

where  $T_I$  satisfies

$$k_I \frac{(T_1 - T_I)}{h_I/2n} = k_s \frac{(T_I - T_0)}{h_s/2}.$$

At the top of the snow, a surface temperature  $T_s$  is obtained from a flux balance condition in which the blackbody emission term is linearly approximated. We let the imposed fluxes of latent heat, sensible heat, incoming solar radiation, and incoming longwave radiation be denoted by  $F_l, F_t, F_r$  and  $F_L$ , respectively. If  $T_p$  is the surface temperature at a previous time step, when the various fluxes were only slightly different, then the current temperature  $T_s$  can be obtained as  $T_s = T_p + \Delta T$ , where  $\Delta T$  satisfies the equation

$$F_l + F_t + F_L + (1 - \alpha_s)F_r + \sigma(T_p)^4 + 4\sigma(T_p)^3\Delta T + k_s \frac{(T_0 - T_p - \Delta T)}{h_s/2} = 0.$$

In case there is no snow on the ice, then the surface ice temperature  $T_I$  is given by  $T_I = T_p + \Delta T$ , where

$$F_l + F_t + F_L + (1 - \alpha_I)(1 - I_0)F_r + \sigma(T_p)^4 + 4\sigma(T_p)^3\Delta T + k_I \frac{(T_1 - T_p - \Delta T)}{h_I/2n} = 0.$$

In the previous two equations,  $\alpha_s$  and  $\alpha_I$  are the albedos of snow and ice, respectively, and  $I_0$  is the fraction of the net incoming solar radiation which penetrates into the interior of snow-free ice.

It should be noted that a more accurate determination of surface temperature can be obtained by iterating the previous process several times. This has not been found to be necessary when the time scale of the applied forcing is very large compared to the time step, but it might be advisable to use iteration when variability exists on short time scales.

In case the predicted snow surface temperature  $T_s$  is above the melting point of  $0^\circ\text{C}$ ,  $T_s$  must be reset to  $0^\circ\text{C}$ ; in this case an imbalance exists between the net upward flux to the atmosphere

$$F_A = F_I + F_L + (1 - \alpha_s)F_r + \sigma(T_s)^4$$

and the conductive flux in the snow

$$F_s = k_s \frac{(T_0 - T_p)}{h_s/2}$$

The thickness of snow then changes in a time step  $\Delta t$  by the negative increment

$$\Delta h_s = \Delta t(F_A - F_s)/q_s,$$

where  $q_s = 26.2 \text{ cal cm}^{-3}$ . Similar considerations apply when snow-free ice is melting: the uppermost grid box changes thickness by an amount

$$\Delta h_I = \Delta t(F_A - F_s)/q_I,$$

with  $q_I = 72 \text{ cal cm}^{-3}$  and  $F_A$  appropriately defined for ice.

At the bottom of the ice, ablation or accretion can change the thickness of the lowermost grid box by

$$\Delta h_B = \Delta t(F_n - F_B)/q_B,$$

where  $q_B = 64 \text{ cal cm}^{-3}$  is the heat of fusion at the lower surface and  $F_B$  is a specified oceanic heat flux.

It remains to describe how temperature is predicted in each grid box and how uniform spacing of temperature points in ice is reestablished after mass changes at the upper and lower boundaries. For the snow layer, the temperature change is given by

$$\Delta T_0 = \begin{cases} \Delta t(F_0 - F_A)/h_s(\rho c)_s, & \text{if } T_s < 0 \\ \Delta t(F_0 - F_s)/(h_s + \Delta h_s)(\rho c)_s, & \text{if } T_s = 0. \end{cases}$$

This is simply a budget equation; and in the case of melting, a temperature budget is applied only to the portion of snow that does not melt. Temperature prediction within the ice is carried out by the rule

$$\Delta T_k = \Delta t \frac{(F_k - F_{k-1})}{(\rho c)_I h_I/n} \quad \text{for} \quad \begin{cases} k=1 & \text{when } h_s \neq 0 \\ k=2, \dots, n-1 \\ k=n & \text{when } \Delta h_B > 0. \end{cases}$$

If  $h_s = 0$ , the uppermost ice layer ( $k=1$ ) is treated

analogously to the snow layer, as is the lowermost layer ( $k=n$ ) when ice ablation ( $\Delta h_B < 0$ ) is occurring. When  $\Delta h_B > 0$ , a new layer of temperature  $T_B$  and thickness  $\Delta h_B$  is added temporarily to the layer structure.

If there is no snow on the ice, the flux of penetrating solar radiation, given by  $F_{I_0} = I_0(1 - \alpha_I)F_r$ , is accumulated in an internal heat reservoir. Whenever the upper-layer ice temperature  $T_1$  would otherwise be below freezing, heat from this reservoir is released to keep  $T_1$  at  $-0.1^\circ$ , unless the reservoir is exhausted.

After the previously described prediction of thickness changes and temperatures in the ice, new grid boxes of thickness  $(h_I + \Delta h_I + \Delta h_B)/n$  are formed. Each of these boxes is composed of portions of at most two of the original boxes of unequal thickness, and a proportional weighting of temperatures in the original boxes is used to obtain temperatures in the new boxes. This simple method restores the uniform spacing in a manner which conserves the total heat content of the ice.

A few remarks are in order about the stability of the preceding numerical scheme. In the present study, a time step  $\Delta t$  of 8 h was selected. (This was chosen because it is compatible with that of a typical ocean model having resolution of several hundred kilometers.) The forward time-differencing should be stable until the grid-box thickness becomes less than  $[2k_s \Delta t / (\rho c)_s]^{1/2} \approx 15 \text{ cm}$  in the snow, or  $[2k_I \Delta t / (\rho c)_I]^{1/2} \approx 25 \text{ cm}$  in the ice. To insure stability in the snow layer, no internal snow temperature is predicted when snow thickness drops below 15 cm. Instead, a vertically constant heat flux, consistent with the surface balance equation, is assumed between the top of the snow and the  $T_1$  point in the ice. If the thickness of individual ice layers drops below 25 cm, the number of layers is reduced, and temperatures in the new layers are obtained by interpolation as above. When ice is less than 25 cm thick, the system of snow and ice is treated by simple mass-budget equations, as described in the Appendix.

In order to summarize this section on the numerical scheme, we reiterate the basic operations involved in carrying out one time step:

- (i) determination of equilibrium surface temperature
- (ii) calculation of surface melting (if any)
- (iii) addition of snowfall (if any)
- (iv) calculation of bottom accretion or ablation
- (v) prediction of the amount of heat stored in brine pockets
- (vi) prediction of temperatures in each grid box
- (vii) interpolation of temperatures to a new grid with uniform spacing
- (viii) reduction in the number of layers (if necessary for computational stability).

#### 4. Specification of standard forcing

A standard forcing is prescribed which is identical to that of Maykut and Untersteiner. In this way, predic-

TABLE 1. Prescribed standard forcing (according to Maykut and Untersteiner, 1969).

Symbol	Variable	Jan	Feb	Mar	Apr	May	Jun	Jul	Aug	Sep	Oct	Nov	Dec	Year
$-F_r$	Incoming short-wave radiation (kcal cm <sup>-2</sup> )	0	0	1.9	9.9	17.7	19.2	13.6	9.0	3.7	0.4	0	0	75.4
$-F_L$	Incoming long-wave radiation (kcal cm <sup>-2</sup> )	10.4	10.3	10.3	11.6	15.1	18.0	19.1	18.7	16.5	13.9	11.2	10.9	166.0
$-F_t$	Flux of sensible heat (kcal cm <sup>-2</sup> )	1.18	0.76	0.72	0.29	-0.45	-0.39	-0.30	-0.40	-0.17	0.10	0.56	0.79	2.71
$-F_l$	Flux of latent heat (kcal cm <sup>-2</sup> )	0	-0.02	-0.03	-0.09	-0.46	-0.70	-0.64	-0.66	-0.39	-0.19	-0.01	-0.01	-3.20
$\alpha_s$	Snow albedo	—	—	0.83	0.81	0.82	0.78	0.64	0.69	0.84	0.85	—	—	—

tions of the simplified model can be verified against those already carried out by M&U for the standard forcing and some 24 variations.

Monthly averaged values of  $F_i$ ,  $F_l$ ,  $F_L$  and  $F_r$  are taken from Fletcher (1965). These fluxes are interpolated using a cubic polynomial through the nearest four monthly values to obtain instantaneous values. Monthly values of snow albedo are taken from Marshunova (1961). These quantities are shown in Table 1, as taken from M&U.

The albedo of ice is set at 0.64 and the fraction of penetrating solar radiation is set at 0.17. The albedo of melting snow is assumed to decrease linearly with snow thickness from the snow albedo at the onset of melting to that of bare ice at the end of melting. The oceanic heat flux  $F_B$  under the ice is specified as 1.5 kcal cm<sup>-2</sup> year<sup>-1</sup>. Snowfall is taken to consist of a linear accumulation of 30 cm between 20 August and 30 October, 5 cm more between 1 November and 30 April, and 5 cm more in May. Snowfall accumulates only when the surface temperature is below freezing.

Maykut and Untersteiner use a value of  $\sigma = 1.385 \times 10^{-12}$  erg cm<sup>-2</sup> K<sup>-4</sup> s<sup>-1</sup> for the Stefan-Boltzmann constant (Maykut, personal communication). This value is about 2% higher than the generally tabulated one; however, we use it here for consistency with M&U. The effect is to make the ice somewhat thicker than it would be if the correct value of  $\sigma$  were used. Since incoming and outgoing longwave fluxes are almost equal and opposite, and since they generally dominate the surface flux balance, one can think of the physical results in Section 6 as more representative of the situation in which incoming longwave fluxes are 2% smaller than those given in Table 1.

### 5. A test of vertical resolution

Prior to making any comparisons with the M&U predictions, the effect of specifying different numbers of temperature points in the ice was examined. Forcing was simplified by eliminating penetrating radiation ( $I_0 = 0$ ) and oceanic heat flux ( $F_B = 0$ ). The yearly snowfall was set at zero, but the surface ice albedo was increased to 0.75 when the surface temperature fell below  $-0.1^\circ\text{C}$ . Thus, only the effect of vertical resolution on

a time-dependent diffusion process in a single medium was considered.

Fig. 2 shows the effect of varying the number of layers  $n$  on the yearly cycle of ice thickness. The curves are essentially equilibrium curves, obtained from 30-year integrations from an initial thickness of 300 cm. The curve for  $n=2$  is already near an asymptotic limit. Curves for  $n=3$  through  $n=9$  (not shown) deviate no more than 5 cm from this curve. An error of about 40 cm occurs when  $n=0$ , by which is meant that no temperature points at all lie within the ice. In such a case, ice thickness is predicted from an assumed linear profile throughout the ice, consistent with the surface flux balance equation.

It appears that the vertical diffusion process in ice about 300 cm thick can be treated quite accurately with two temperature points in the ice. This number is used in subsequent calculations, and the complete model, with snow cover included, is called the "3-layer model." (The possibility of using only one internal

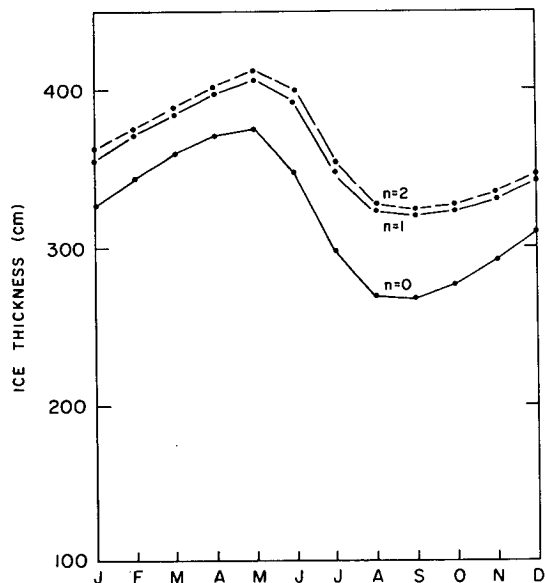


FIG. 2. Effect of the number of layers  $n$  used in predicting the annual cycle of ice thickness under simplified forcing. For  $n=0$ , only a mass budget equation is used. The case  $n=2$  is near an asymptotic limit.

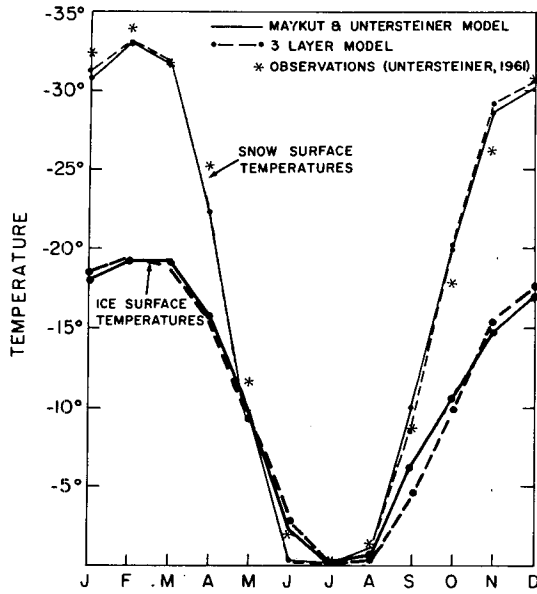


FIG. 3. Temperatures at the snow surface and the ice surface, as predicted by the M&U and the 3-layer models for standard forcing.

temperature point in the ice is ruled out because the energy of penetrating radiation might then be applied at too deep a level within the ice.)

6. Some selected integrations

In this section, predictions based on 65-year integrations of the 3-layer model are compared with those of Maykut and Untersteiner (1969) for a variety of en-

vironmental conditions. The primary emphasis is on the degree of comparison, rather than on the physical basis of the response. Readers interested in more detail on the latter question may want to refer to the discussion in the M&U papers.

Fig. 3 shows the predicted monthly average temperature at the snow surface and at the snow-ice interface, in the case of standard forcing. The snow surface temperature is the more important of the two, as far as interaction with the atmosphere is concerned. The two models are quite consistent with each other and with the observations of Untersteiner (1961). There is almost as good agreement between the predicted temperatures at the snow-ice interface. The largest difference in temperatures at this interface occurs in September; this indicates that the 3-layer model stores more heat internally in brine pockets than does the M&U model. (In fact, heat which is stored only implicitly by a temperature-dependent heat capacity in the M&U model is lost from the upper layers that melt during the summer.)

The size of the temperature discrepancies in Fig. 3 is typical of those occurring in other cases. Henceforth, we concentrate only on a comparison of the ice thickness predictions of the two models.

Fig. 4 shows the monthly average ice thicknesses for five paired cases. Variations in the oceanic heat flux from 0.0 to 4.5 kcal cm<sup>-2</sup> year<sup>-1</sup> are seen to cause the annual average ice thickness to change by a factor of 5. The two models give consistent results over this wide range of response. (The value  $F_B = 1.5$  is the "standard" forcing.)

Fig. 5 depicts the ice thickness in four more paired experiments, in which the fraction  $I_0$  of penetrating radiation and ice albedo  $\alpha_I$  are varied. Mean annual thickness increases as more radiation is allowed to be stored in brine pockets and released gradually at a later time. A reduction in ice albedo from 0.64 to 0.58

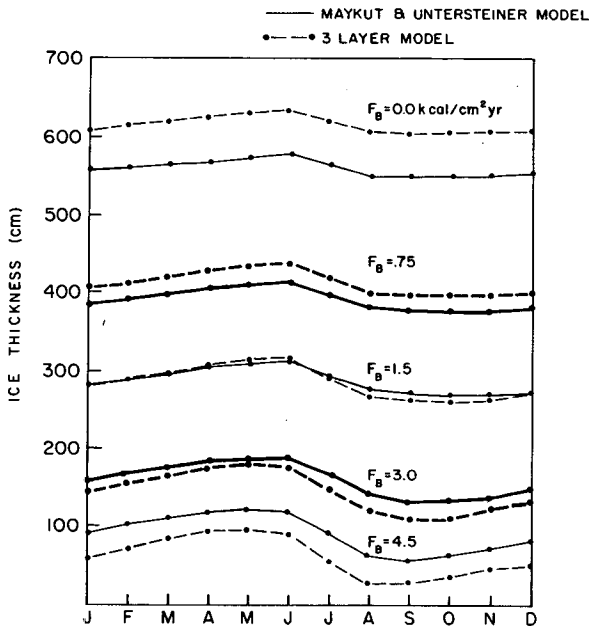


FIG. 4. Comparison of annual thickness cycles for different specifications of oceanic heat flux.

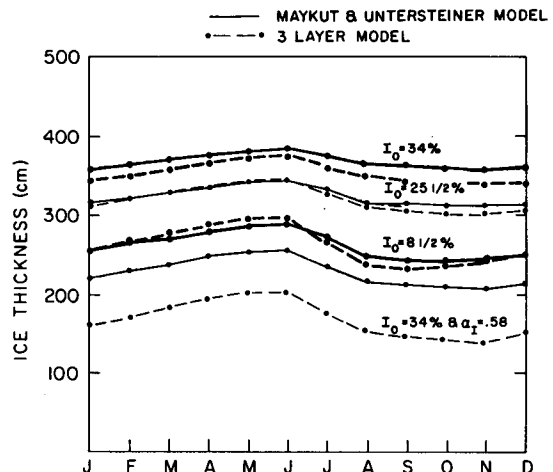


FIG. 5. Comparison of annual thickness cycles for different values of penetrating solar radiation  $I_0$  and ice albedo  $\alpha_I$ .

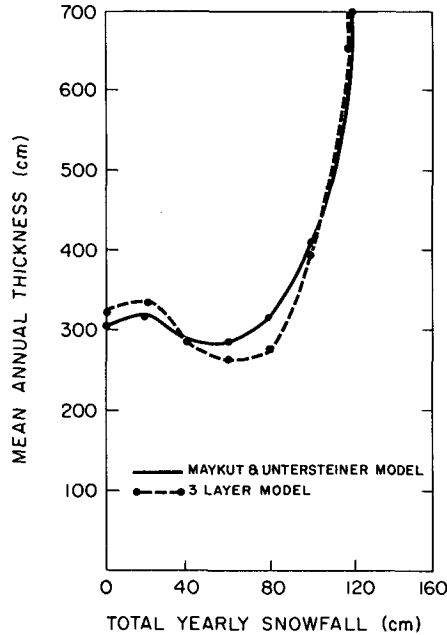


FIG. 6. Effect of total yearly snowfall on mean annual ice thickness predicted by the two models.

causes a significant decrease in ice thickness. The similar response of the two models suggests that the simple heat-storage mechanism in the 3-layer model captures the essential physics of internal melting and refreezing. The relatively thicker ice predicted by the M&U model for large  $I_0$  values is probably due to the smaller internal heat storage referred to earlier.

The effect on mean annual ice thickness caused by varying the total yearly amount of snowfall is shown in Fig. 6. Both models show a gradual tendency for ice thickness to decrease initially on account of the insulating effect of increasing snow cover. Both models also show an abrupt rise in ice thickness as a limiting value of snowfall is reached, beyond which the ice remains snow-covered throughout the year. The limiting value of snowfall for the 3-layer model is nearly the same as that for the M&U model.

The effects of miscellaneous other changes in forcing are shown in Fig. 7. Both models predict increases in mean annual ice thickness when oceanic salinity decreases (thereby increasing  $T_B$ ) or when atmospheric fluxes from Vowinckel and Orvig (1966, 1967) are prescribed. Both models predict moderate reductions in ice thickness when (i) no radiation penetrates into the ice ( $I_0=0$ ), (ii) solar radiation  $F_s$  increases by 10%, or (iii) incoming longwave radiation  $F_L$  is 10% higher during fall and winter. Finally, both models call for substantial reductions in ice thickness if no turbulent fluxes are allowed or if the summer albedo drops by 0.1. In the last case, the simplified model predicts appearance of open water in summertime; but since ice reappears for the remainder of the year, a mean

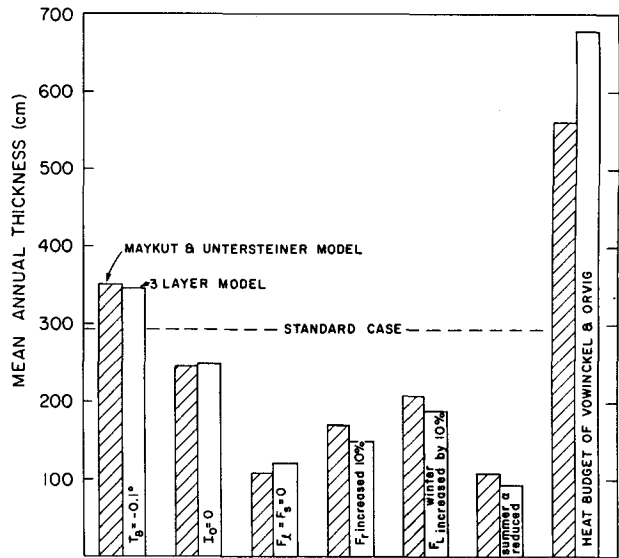


FIG. 7. Effects of other parameter variations on mean annual ice thickness predicted by the two models.

annual ice thickness can still be computed for comparison with the M&U results.

In three cases, Maykut and Untersteiner predict "no ice." This means that open water occurred at some point of each time integration and the experiment was terminated. In the 3-layer model, open water occurs periodically, but continued integration shows that thin ice is present each winter. This happens when (i) oceanic heat flux of  $6 \text{ kcal cm}^{-2} \text{ year}^{-1}$  is specified, (ii) summer albedo is reduced by 0.2, or (iii) both the atmospheric fluxes and the albedo from Vowinckel and Orvig (1966, 1967) are used.

An interesting feature of the 3-layer predictions of open water is that *multi-year* cycles of ice thickness can occur. These cycles repeat themselves exactly, and open water may appear only once in each multi-year period (see Fig. 8). This phenomenon is made possible by the differing conductivities of snow and ice. Following the appearance of open water in a given summer, the ocean

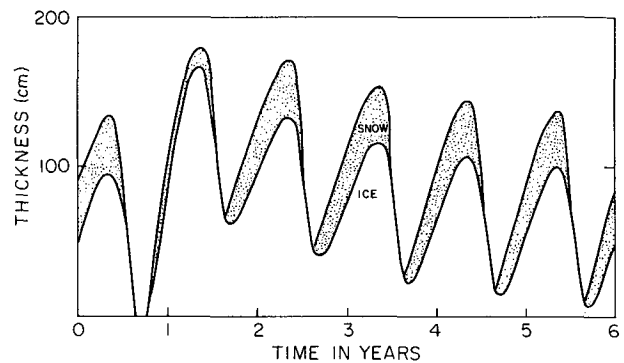


FIG. 8. A multi-year equilibrium cycle of ice thickness, as predicted by the 0-layer model (cf. Appendix) for the case in which oceanic heat flux is  $6 \text{ kcal cm}^{-2} \text{ year}^{-1}$ . Similar cycles occur in the 3-layer model.

TABLE 2. Summary of cases run (adapted from Maykut and Untersteiner, 1969).

Case no.	3-layer mean annual thickness (cm)	Maykut and Untersteiner mean annual thickness (cm)	Characteristics
1	287	288	Fletcher's heat budget and $F_B = 1.5 \text{ kcal cm}^{-2} \text{ year}^{-1}$ (the "standard case")
2	not applicable	310	Uniform, low ice salinity (0.09 ‰)
3	not applicable	99	Uniform, low ice salinity (0.09 ‰) and $F_B = 4.5 \text{ kcal cm}^{-2} \text{ year}^{-1}$
4	343, for $T_B$ change only	349	Uniform, low ice salinity (0.09 ‰) and near-fresh water ( $-0.1^\circ\text{C}$ ) below the ice
5	no ice	no ice	Vowinckel/Orvig heat budget and albedo
6	680	560	Vowinckel/Orvig heat budget and albedo of Marshunova (Table 1)
7	245	243	$I_0 = 0\%$ of $F_r$ ; no fraction of the shortwave radiation penetrating the ice surface
8	262	262	$I_0 = 8.5\%$ of $F_r$ during snow-free period
9	320	324	$I_0 = 25.5\%$ of $F_r$ during snow-free period
10	351	368	$I_0 = 34.0\%$ of $F_r$ during snow-free period
11	168	229	$I_0 = 34.0\%$ of $F_r$ during snow-free period and ice albedo lowered to 0.58
12	619	561	$F_B = 0$ ; no heat flux in the ocean
13	415	391	$F_B = 0.75 \text{ kcal cm}^{-2} \text{ year}^{-1}$
14	146	162	$F_B = 3.0 \text{ kcal cm}^{-2} \text{ year}^{-1}$
15	61	93	$F_B = 4.5 \text{ kcal cm}^{-2} \text{ year}^{-1}$
16	no ice	no ice	$F_B = 6.0 \text{ kcal cm}^{-2} \text{ year}^{-1}$
17	322	305	No snow ( $h_{\max} = 0$ ); ice albedo = 0.75 if below $272.9 \text{ K}$ surface temperature
18	338	319	$h_{\max} = 20 \text{ cm}$
19	266	283	$h_{\max} = 60 \text{ cm}$
20	277	317	$h_{\max} = 80 \text{ cm}$
21	395	411	$h_{\max} = 100 \text{ cm}$
22	660	702	$h_{\max} = 120 \text{ cm}$
23	119	107	$F_s = F_l = 0$ ; no flux of sensible or latent heat
24	145	169	$F_r$ increased by 10%
25	186	203	$F_L$ (incoming longwave) increased by 10% during October–April
26	no ice ( $h = 90$ )	105	Albedo reduced by 0.1 during June–August
27	no ice	no ice	Albedo reduced by 0.2 during June–August

does not refreeze until after the heavy snowfall season. With a thinner cover of insulating snow, the ice grows rapidly during the subsequent winter to such a thickness that several years with the usual snow cover must pass before open water reappears. This mechanism might be important in causing multi-year anomalies in the observed ice cover.

## 7. Discussion

The results of the previous paired integrations are summarized in Table 2. With the exception of two M&U cases for ice of low salinity, their entire series of environmental changes has been examined. As is evident from the table, agreement between the two models is generally excellent. Three-fourths of the cases agree within 24 cm. Even better agreement would probably exist if there were no differences in the treatment of internal heat storage by brine pockets. For all 25 cases, the average absolute error is only 22 cm.

The model of Maykut and Untersteiner is a carefully formulated and comprehensive treatment of sea ice thermodynamics. In the absence of observational data on the response of sea ice to changes in climatic forcing, their model has been used as the standard against which to test a simplified model. Without their previous work, estimating the validity of a simplified model would be a much harder task.

The present study has concentrated on a comparison of two models. A few final modifications can be made to prepare the 3-layer model for climate studies. The formulation of the albedo of melting snow could be simplified so that the albedo and thickness at the onset of melting don't have to be retained. Also, the heats of fusion  $q_I$  and  $q_B$  at the upper and lower ice boundaries should be made identical. Otherwise there will be fictitious implied sinks of heat in a model, associated with alternating surface melting and bottom accumulation. In addition, it might be appropriate to specify



different values of ice albedo and ice conductivity when the ice is very thin.

Another modification which should be considered is the inclusion of the open water in leads as a predicted variable in the model. A very simple method of doing this is being tested in collaboration with other investigators (cf. Washington *et al.*, 1976); and initial results are promising. The method is based on three basic assumptions:

1) In each geographical area, a small fraction of the ocean surface (on the order of 1%) always remains ice-free, regardless of cooling, on account of short-term variations in wind forcing or long-term divergences in wind forcing.

2) Any excess of heat absorbed in leads during spring or summer increases the fractional area of open water by laterally melting ice at its existing thickness.

3) Any net loss of heat from those leads which exceed the minimum allowable area increases the area of ice by formation of new thin ice and by a reduction of the mean thickness to the area-weighted average of old thick ice and new thin ice.

By means of the above assumptions, at least some qualitative features can be modelled, whereby open areas enlarge rather slowly by melting old thick ice but freeze over rapidly by formation of new thin ice. The main difficulty in a quantitative sense may be the specification of a minimum amount of open water, which exists as a result of dynamical processes not included in the prediction.

The 3-layer model requires machine storage at each point of two thicknesses, three layer temperatures, the heat stored in brine pockets, and the surface temperature (the last being an estimate for the next surface equilibrium value). Since the forward time stepping requires retention of only one time-level in memory, the storage requirement is about the same as holding velocity, temperature and salinity at two time levels for one layer of ocean in the polar regions. Computation time should be less than for one layer of ocean, because equal time steps can be used and the number of computer operations per time step is probably smaller in the ice model. (If storage space and computer time are severely limited, one can employ an even simpler model, as described in the Appendix.)

In summary, the model developed in this study would appear to provide three advantages for predicting thermodynamic growth of sea ice in climate studies. As has already been said, it is reasonably fast and it is accurate over a wide range of forcing. A final advantage to keep in mind is that its response to typical sorts of forcing is known. Anomalous behavior in climatic ice predictions can therefore be attributed to deficiencies in components of the system other than sea ice.

*Acknowledgments.* The author wishes to thank B. Gladstone for drafting the figures and G. Jones and S.

Lovell for typing the manuscript. Helpful suggestions during the model development were made by W. L. Gates, G. A. Maykut and R. C. Alexander. This work was carried out under Contract DAHC 15 73 C 0181 for the Defense Advanced Research Projects Agency.

## APPENDIX

### An Even Simpler Model for Sea Ice Thermodynamics

For some applications of climate modeling, even a 3-layer ice model may be too cumbersome in terms of computation time and machine storage. If one is willing to tolerate somewhat greater errors in predictions of seasonal ice thickness, while still obtaining reasonable values for mean annual thickness, a simpler model can be used.

The model has only three prognostic variables: snow thickness  $h_s$ , ice thickness  $h_I$ , and surface temperature  $T_s$ . The surface temperature is the equilibrium value that would result if the internal snow and ice temperature structure adjusted instantaneously to external forcing. For snow-covered ice, the resulting uniform heat flux in both ice and snow is given by

$$F_s = \frac{k_s(T_B - T_s)}{h_s + (h_I k_s / k_I)},$$

whereas for snow-free ice the flux is given by

$$F_s = k_I \frac{(T_B - T_s)}{h_I}.$$

The surface temperature is obtained from setting

$$F_s + F_A = 0, \quad (\text{A1})$$

where the net heat flux  $F_A$  upward to the atmosphere is defined in Section 3. This equation can be solved for  $T_s$  in the same manner as before, using the equilibrium temperature  $T_p$  of the previous time step in a linearized form of the blackbody emission term in  $F_A$ . (Note that the surface temperature could also be found by a Newton-Raphson iterative process, if only the variables  $h_s$  and  $h_I$  are carried in memory.)

If the equilibrium surface temperature derived from Eq. (A1) is above the melting point, then surface melting is determined by recomputing  $F_A$  and  $F_s$  for  $T_s = 0$  and setting

$$\Delta h_s = \Delta t (F_A - F_s) / q_s \quad \text{for snow-covered ice}$$

or

$$\Delta h_I = \Delta t (F_A - F_s) / q_I \quad \text{for snow-free ice.}$$

Ablation or accretion of ice at the lower boundary is given by

$$\Delta h_B = \Delta t (F_s - F_B) / q_B.$$

In Section 5, it was noted that the assumption of a linear equilibrium profile of temperature causes ice

thickness to be too small by about 12%, even when there is no fraction  $I_0$  of penetrating radiation. An amount of heat that normally must be removed from the ice in early fall is neglected, as is a larger amount of heat that must be added to the thicker ice in late spring. Because a net positive amount of heat that would normally warm the interior of the ice goes into additional melting, the ice is thinner than it should be. To compensate for this error, the conductivities  $k_s$  and  $k_I$  of snow and ice are increased by a factor  $\gamma$ , so that additional winter ice growth will offset the extra summer melting. A choice of  $\gamma=1.065$  brings the predicted mean annual ice thickness for Case 7 (in which there is no penetrating radiation) into agreement with the M&U value.

A fraction  $I_0$  of penetrating radiation would normally cause an increase in brine volume and subsequently retard cooling near the upper surface of the ice. In this extremely simplified model, a portion  $\beta < 1$  of the radiation that would usually penetrate the ice is reflected away, while the remaining portion  $(1-\beta)$  is applied as surface energy flux. Thus, the albedo of the ice is effectively increased to

$$\alpha = \alpha_I + \beta(1 - \alpha_I)I_0.$$

A value for the parameter  $\beta=0.4$  is chosen to make the mean annual ice thickness for Case 1 (the standard

TABLE 3. Equilibrium ice thickness (cm) for various thermodynamic models.

Case no.	3-layer model	M&U model	0-layer model
1	287	288	289
2	NA	310	NA
3	NA	99	NA
4	343	349	333
5	no ice	no ice	no ice
6	680	560	573
7	245	243	243
8	262	262	264
9	320	324	319
10	351	368	352
11	168	229	216
12	619	561	504
13	415	391	376
14	146	162	172
15	61	93	97
16	no ice	no ice	no ice
17	322	305	333
18	338	319	320
19	266	283	275
20	277	317	283
21	395	411	330
22	660	702	470
23	119	107	148
24	145	169	177
25	186	203	209
26	no ice ( $\bar{h}=90$ )	105	no ice ( $\bar{h}=94$ )
27	no ice	no ice	no ice

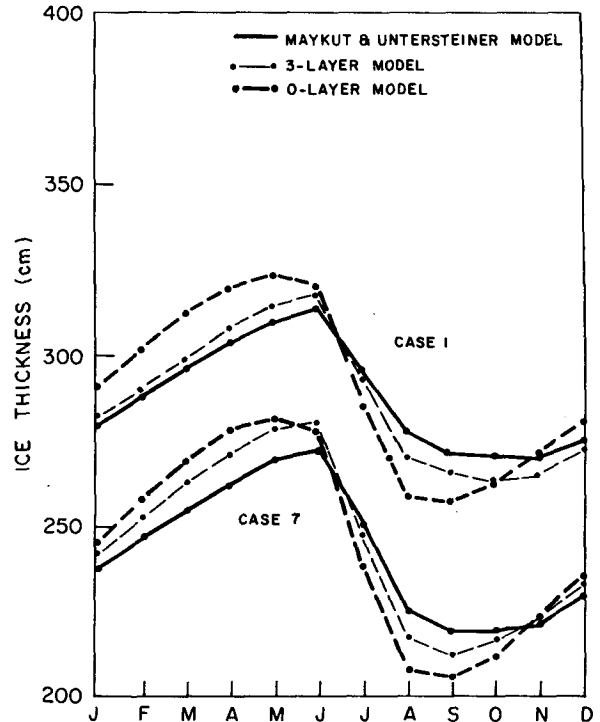


Fig. 9. Annual thickness cycles of three ice models for the cases of 0% and 17% penetrating radiation.

case with 17% penetrating radiation) agree in the two models.

The thickness predictions of the simple model with fixed values of  $\gamma=1.065$  and  $\beta=0.4$  can be computed for the remaining 23 cases of M&U. The results are shown in Table 3, where the extremely simple model is called the "0-layer model." In three-fourths of the cases, mean annual thicknesses agree with those of Maykut and Untersteiner within 16 cm. The average absolute error in all cases is 24 cm. Thus the 0-layer model performs essentially as well as the 3-layer model in predicting near annual thicknesses. However the amplitude and phase of the seasonal variation are somewhat distorted (see Fig. 9). The 0-layer model is less accurate in some respects than the 3-layer model, but may be preferable if computer speed and storage allocation are important considerations.

The 0-layer formulation is used in the 3-layer model whenever ice thickness is less than 25 cm. Adjustment time-scales are very short for such thin ice, and the equilibrium assumption should be very nearly correct. When used in this context, the fraction  $I_0$  of penetrating radiation is taken to be zero, and no increase in conductivity is made.

REFERENCES

Fletcher, J. O., 1965: The heat budget of the Arctic Basin and its relation to climate. The Rand Corporation, Santa Monica, Calif., R-444-PR.

- Marshunova, M. S., 1961: Principal characteristics of the radiation balance of the underlying surface and of the atmosphere in the Arctic. *Proc. Arctic and Antarctic Res. Institute*, No. 229, Leningrad [Translated by the Rand Corporation, RM-5003-PR, 1966].
- Maykut, G. A., and N. Untersteiner, 1969: Numerical prediction of the thermodynamic response of Arctic sea ice to environmental changes. The Rand Corporation, Santa Monica, Calif., RM-6093-PR.
- , and —, 1971: Some results from a time-dependent, thermodynamic model of sea ice. *J. Geophys. Res.*, **76**, 1550–1575.
- Untersteiner, N., 1961: On the mass and heat budget of Arctic sea ice. *Arch. Meteor. Geophys. Bioklim.*, **A12**, 151–182.
- Vowinkel, E., and S. Orvig, 1966: Energy balance of the Arctic. V: The heat budget of the Arctic Ocean. *Arch. Meteor. Geophys. Bioklim.*, **14**, 303–325.
- , and —, 1967: Climate change over the Polar Ocean. I: The radiation budget. *Arch. Meteor. Geophys. Bioklim.*, **15**, 1–23.
- Washington, W., A. Semtner, C. Parkinson and L. Morrison, 1976: On the development of a seasonal change sea ice model. (Submitted for publication).